

1 **Persistent kallikrein5 activation induces atopic dermatitis-like skin**  
2 **architecture independent of PAR2 activity**

3 Yanan Zhu<sup>1</sup> PhD, Joanne Underwood<sup>2</sup> PhD, Derek Macmillan<sup>3</sup> PhD, Leila Shariff<sup>3</sup> PhD, Ryan  
4 O'Shaughnessy<sup>1</sup> PhD, John I. Harper<sup>1</sup> MD FRCP FRCPCH, Chris Pickard<sup>2</sup> PhD, Peter S.  
5 Friedmann<sup>2</sup> MD FRCP FMedSci, Eugene Healy<sup>2,4</sup> MB PhD FRCP FRSB , Wei-Li Di<sup>1</sup> MBBS PhD

6  
7 1. Infection, Immunity, Inflammation and Physiological Medicine Programme, Immunobiology  
8 Section, UCL Institute of Child Health, 30 Guildford Street, London WC1N 1EH, UK.

9 2. Dermatopharmacology, Sir Henry Wellcome Laboratories, Faculty of Medicine, University of  
10 Southampton, Southampton General Hospital, SO16 6YD, UK

11 3. Department of Chemistry, University College London, 20 Gordon Street, WC1H 0AJ, UK.

12 4. Dermatology, University Hospital Southampton NHS Foundation Trust, Southampton, SO16  
13 6YD, UK

14 **Corresponding Author:**

15 Dr. Wei-Li Di, MBBS, PhD

16 Senior Lecturer,

17 UCL Institute of Child Health, Immunobiology Section,

18 30 Guildford Street, London WC1N 1EH, UK.

19 Tel: 44 (0)20 79052369

20 Fax: 44 (0)20 78138494

21 E-mail [w.di@ucl.ac.uk](mailto:w.di@ucl.ac.uk)

22 **Conflicts of interest:**

23 none

24 **Declaration of source of funding:**

25 Funding for the study was supported by Sparks and the Livingstone Fund [Great Ormond Street  
26 Hospital Children's Charity] and BBSRC.

27 **Abstract**

28 **Background:** Up-regulation of kallikreins (KLK) including KLK5 has been reported in atopic  
29 dermatitis (AD). KLK5 has biological functions which include degrading desmosomal proteins and  
30 inducing pro-inflammatory cytokine secretion through protease activated receptor 2 (PAR2).  
31 However, due to the complex interactions between various cells in AD inflamed skin, it is difficult  
32 to dissect the precise and multiple roles of up-regulated KLK5 in AD skin.

33 **Objective:** We investigated the effect of up-regulated KLK5 on the expression of epidermal related  
34 proteins and cytokines in keratinocytes and on skin architecture.

35 **Methods:** Lesional and non-lesional AD skin biopsies were collected for analysis of morphology  
36 and protein expression. The relationship between KLK5 and barrier related molecules was  
37 investigated using an *ex-vivo* dermatitis skin model with transient KLK5 expression and a cell  
38 model with persistent KLK5 expression. The influence of up-regulated KLK5 on epidermal  
39 morphology was investigated using an *in vivo* skin graft model.

40 **Results:** Up-regulation of KLK5 and abnormal expression of desmoglein 1 (DSG1) and filaggrin  
41 (FLG), but not PAR2 were identified in AD skin. PAR2 was increased in response to transient up-  
42 regulation of KLK5, while persistently up-regulated KLK5 did not show this effect. Persistently up-  
43 regulated KLK5 degraded DSG1 and stimulated secretion of IL-8, IL-10 and TSLP independent of  
44 PAR2 activity. With control of higher KLK5 activity by the inhibitor SFTI-G, restoration of DSG1  
45 expression and a reduction in AD-related cytokine IL-8, TLSP and IL-10 secretion were observed.  
46 Furthermore, persistently elevated KLK5 could induce AD-like skin architecture in an *in vivo* skin  
47 graft model. .

48 **Conclusion:** Persistently up-regulated KLK5 resulted in AD-like skin architecture and secretion of  
49 AD-related cytokines from keratinocytes in a PAR-2 independent manner. Inhibition of KLK5-  
50 mediated effects may offer potential as a therapeutic approach in AD.

51

52

53 **Key messages**

- 54 • Persistently up-regulated KLK5 induces PAR2-independent IL-8, IL10 and TSLP secretion,  
55 causing abnormal keratinocyte growth and AD-like skin architecture.
- 56 • Inhibition of KLK5-mediated effects restored DSG1 expression and decreased AD-related  
57 cytokine expression, thus suggesting that KLK5 inhibition may be useful as a potential  
58 treatment for AD.

59

60 **Capsule summary**

61 Persistently increased serine protease kallikrein 5 modifies skin barrier proteins, upregulates AD-  
62 related cytokine expression and induces AD-like skin architecture. Inhibition of KLK5 may offer  
63 potential as a treatment strategy in AD.

64

65 **Key word**

66 Kallikrein 5, atopic dermatitis, skin barrier, serine protease inhibitor, SFTI

67

68 **abbreviations**

69 KLK5 (kallikrein), DSG1 (desmoglein 1), PAR2 (protease activated receptor 2), CAP18  
70 (cathelicidin precursor cationic antimicrobial protein 18), AD (atopic dermatitis), NS (Netherton  
71 syndrome), FLG (filaggrin), UT (untransduced keratinocytes), AP (PAR2 agonist), TSLP (thymic  
72 stromal lymphopoietin), rKLK5 (recombinant KLK5).

73

74

75

76

77

## 78 **Introduction**

79 Tissue kallikreins (KLKs) are a family of fifteen (chymo)trypsin-like serine proteases which  
80 function through proteolytic cascades in the skin. Eight KLKs are expressed in the skin with KLK5  
81 being one of the three most important, the others being KLK7 and KLK14<sup>1</sup>. KLK5 is produced as  
82 an inactive precursor from keratinocytes and activated by matriptase and KLK14<sup>2,3</sup>, but can also  
83 undergo self-activation. It is able to activate other KLKs, therefore, KLK5 has been considered to  
84 be the initiator of KLK activation cascades within the skin<sup>4</sup>.

85 KLK5 is expressed in the outmost layers of the epidermis, and the importance of its biological  
86 function in the epidermal barrier was initially discovered through studies on Netherton Syndrome  
87 (NS), a rare severe autosomal recessive skin disorder caused by mutations in the *SPINK5* gene<sup>4,5</sup>. In  
88 NS, *SPINK5* mutations cause loss of function of its encoded protein LEKTI, a multi-domain serine  
89 protease inhibitor, leading to elevated activity of KLK5. This results in cleavage of intercellular  
90 adhesion protein desmoglein 1 (DSG1), causing excessive desquamation of corneocytes and leading  
91 to a severely defective skin barrier, a major cause of early neonatal death in NS<sup>6</sup>. In addition to its  
92 involvement in DSG1 degradation, KLK5 is able to activate protease activated receptor 2 (PAR2), a  
93 subfamily of G protein-coupled receptors, and trigger expression of pro-inflammatory cytokines  
94 such as IL-8<sup>7,8</sup>. KLK5 is also involved in the innate immune system within the skin by cleaving the  
95 cathelicidin precursor cationic antimicrobial protein 18 (CAP18) at its c-terminus to produce 37  
96 amino acid peptide LL-37, a major antimicrobial peptide with broad-spectrum antimicrobial  
97 activity<sup>9</sup>.

98 Up-regulation of kallikreins including KLK5 has been reported in many chronic inflammatory skin  
99 diseases including atopic dermatitis (AD)<sup>10,11</sup>. AD is a multifactorial disease caused by complex  
100 interactions between genetic and environmental factors, with evidence that irritants (such as those  
101 contained in soaps) can further damage the skin barrier and exacerbate the inflammation in AD  
102 patients<sup>12</sup>. In the past decade, significant progress has been made in the area of molecular genetics  
103 with identification of several genes linked to AD including *SPINK5*, *KLK7* and *FLG*<sup>13-15</sup>. These

104 findings have led to the proposition that an impaired epidermal barrier is the primary event,  
105 allowing percutaneous allergen penetration and causing an enhanced Th2-skewed immune-  
106 response<sup>16</sup>. The induced inflammatory response further compromises barrier function, resulting in  
107 abnormal expression, activity and assembly of skin barrier related proteins, enzymes and lipids.  
108 Aberrant up-regulation of KLK5 in AD skin has been reported<sup>10,11</sup> and increased KLK5 may play a  
109 key role in the pathogenesis of the dysfunctional skin. However, due to the complex interactions  
110 between various cells in AD inflamed skin, it is difficult to dissect the exact role of up-regulated  
111 KLK5 in AD skin.

112 In this study, we confirmed up-regulation of KLK5 and abnormal expression of KLK5 down-stream  
113 molecules DSG1 and filaggrin (FLG), but not PAR2 in AD skin. We also identified significantly  
114 increased KLK5 and PAR2 expressions in an *ex-vivo* dermatitis model, but not in the cell model  
115 with persistent over-expression of KLK5, illustrating different responses of PAR2 to transient or  
116 persistent KLK5 stimulation. We also demonstrated that increased IL-8, IL-10 and TSLP in  
117 keratinocytes with persistently expressed KLK5 was independent of PAR2 activity, and that  
118 inhibition of KLK5 activity with the serine protease inhibitor SFTI-G reduced cytokine production  
119 and normalised DSG1 protein expression. Furthermore, persistent KLK5 over-expression alters  
120 keratinocyte behaviour *in vivo*, resulting in epidermal acanthosis similar to that observed in AD skin,  
121 indicating a key role for KLK5 in AD pathology.

122

123

124

125

126

127

128

129 **Materials and Methods**

130 Skin biopsies and haematoxylin and eosin staining (H&E)

131 Skin biopsies were taken from non-lesional and lesional skin from five AD patients. Five age-  
132 matched healthy donors were also obtained. This study was approved by the local ethics committee  
133 (LREC number 05/Q0508/106). Skin samples were formalin fixed paraffin embedded, and H&E  
134 staining was performed on 6 µm thickness paraffin skin sections using standard histochemistry  
135 techniques.

136

137 Immunostaining and protein quantification

138 Immunofluorescence and immunohistochemistry staining were carried out on frozen or paraffin  
139 embedded tissue sections using a purified anti-KLK5 mouse polyclonal antibody in 1:500 dilutions  
140 (Novus Biologicals, Abingdon, UK), or an anti-DSG1 mouse monoclonal antibody recognizing N-  
141 terminal extracellular domain (clone P124) in 1:100 dilutions (2B Scientific Ltd, Upper Heyford,  
142 UK), or an anti-FLG monoclonal antibody in 1:100 dilutions (Leica biosystems, Newcastle, UK), or  
143 an anti-involucrin mouse monoclonal antibody in 1:1000 (Sigma, Dorset, UK) or an anti-keratin 10  
144 mouse monoclonal antibody (clone number LHP2, a gift from Royal London Hospital, UK).  
145 MolecularProbes secondary antibodies conjugated with fluorescence dye were obtained from Life  
146 Technologies (Paisley, UK). The detection of immunohistochemistry used biotinylated secondary  
147 antibodies and DAB substrate kit for peroxidase (Vector laboratories, Peterborough, UK). The  
148 staining procedures were as described by Di et al<sup>17</sup>, and negative controls were performed in each  
149 staining with the secondary antibody alone.

150 The quantification of protein expression and activity in the epidermis was performed based on the  
151 staining intensity using software Image-Pro Plus v6.0 (Media Cybernetics, Cambridge, UK). Briefly  
152 images of three non-overlapped but adjacent regions in each section were recorded and saved  
153 digitally. The epidermis in each image was then highlighted as an area of interest (AOI) and the  
154 defined positive staining threshold was applied to the AOIs. The optical counts of positive staining

155 within AOIs were automatically counted based on the defined threshold and the expression or  
156 activity in each AOI was calculated as mean staining intensity /area.

157

#### 158 Primary keratinocyte and keratinocyte cell line culture

159 Primary keratinocytes and fibroblasts were isolated from skin biopsies by incubation with 0.25%  
160 trypsin-EDTA (Life Technologies, Paisley, UK) 3 hours for keratinocytes and Serva 50 U/ml  
161 collagenase NB6 (Universal Biologicals, Cambridge, UK) 2 hours for fibroblasts. Isolated primary  
162 keratinocytes were then co-cultured with lethally irradiated 3T3 mouse fibroblasts and grown in  
163 keratinocyte culture media. The media contained equal amount of DMEM and DMEM/Ham F12  
164 (Life Technologies, Paisley, UK) supplemented with 10% FCS (Labtech, East Sussex, UK), 100  
165 IU/ml of penicillin and 100 µg/ml of streptomycin (Life Technologies, Paisley, UK). Human  
166 keratinocyte growth supplement was then added to the media at final concentrations of 10 ng/ml of  
167 EGF (Bio-Rad AbD Serotec, Oxford, UK), 0.4 µg/ml of hydrocortisone, 5 µg/ml of transferrin, 5  
168 µg/ml of insulin,  $2 \times 10^{-11}$  M of liothyronine and  $1 \times 10^{-10}$  M of cholera toxin (Sigma, Dorset, UK).  
169 Ntert<sup>18</sup>, a keratinocyte cell line was cultured in the same keratinocyte media. Fibroblasts were  
170 cultured in DMEM supplemented with 10% FCS, 100 IU/ml of penicillin and 100 µg/ml of  
171 streptomycin.

172

#### 173 Ex-vivo dermatitis model and immunofluorescent staining

174 Skin from female breast tissue, obtained with informed consent and ethical approval (LREC  
175 07/Q1704/59) following mastectomy was used as an *ex vivo* dermatitis model. The skin, which was  
176 surplus to histopathology requirement, was placed in ice cold PBS immediately following removal  
177 and stored on ice for a maximum of 2 hours, then placed into a 60 mm petri dish and the epidermal  
178 surface carefully blotted dry. Rubber O-rings with a diameter of 8 mm were sealed on to the skin  
179 using soft paraffin wax to create wells; care was taken to ensure that paraffin wax was applied only  
180 to the area where the O-ring made contact with the skin in order to avoid altering the permeability

181 of the skin or the protease activity within the epidermis. To prevent the skin from drying out during  
182 the incubation period, the remaining space within the petri dish was filled with DMEM, containing  
183 10% FCS, at a depth of approximately 2 mm, ensuring no medium touched the epidermal surface of  
184 the skin. Irritant substances and appropriate vehicle controls were applied carefully to separate  
185 wells (50 µl solution each) and the skin incubated at 37°C with 5% CO<sub>2</sub> for the required length of  
186 time. Following incubation, the entire irritant and vehicle control solutions were aspirated off the  
187 epidermis and 6 mm punch biopsies were taken from the treated sites of the skin sample (without  
188 removing the rubber O-rings) using sterile biopsy punches. A fresh biopsy punch was used for each  
189 treatment to avoid cross-contamination, and the biopsy was removed from within the rubber O-ring  
190 using forceps to ensure only treated skin was extracted. The biopsied tissue was placed in a 1.5 ml  
191 eppendorf tube and snap frozen in liquid nitrogen. Samples were stored at -80°C until further  
192 investigations.

193 Following removal of skin biopsies from -80°C storage and embedding in Tissue-Tek® optimal  
194 cutting temperature medium (OCT) (Sakura Finetek, Thatchem, UK), 8 µm tissue sections were cut  
195 on a cryostat, allowed to dry onto poly-L-lysine coated glass slides, then fixed for 10 minutes in ice  
196 cold acetone at -20°C. Slides were washed with TBS, blocked for 30 minutes with blocking buffer  
197 followed by incubation with primary antibody in TBS overnight at 4°C. Slides were washed for 3 x  
198 5 minutes in TBS, subsequently incubated with secondary antibody for 1 hour in the dark, then  
199 washed in TBS for 3 x 5 minutes and, where necessary, counterstained by incubation with DAPI for  
200 10 minutes, followed by a final wash of 3 x 5 minutes in TBS. Coverslips were attached using  
201 Mowiol and the samples then visualised by fluorescence microscopy (Axioskop 2 MOT, Zeiss).  
202 Slides were magnified at 100x and 400x and images digitally recorded (Axiocam, Zeiss). Slides  
203 stained in the absence of primary antibody were used to set the exposure levels to reduce  
204 background staining. Images were analysed using ImageJ v1.46 software, with 10 vertical regions  
205 of interest (ROI's) from outer to inner surface of the epidermis selected from 1 field of view from 3  
206 consecutive sections for each sample and the contribution from each layer along this measurement



207 was recorded. The 10 measured ROIs were normalised to 100% and the mean pixel intensity  
208 obtained for every 5% of the depth (i.e. from outer to inner surface) of the epidermis. The minimum  
209 average pixel intensity for a 5% section in the PBS sample was set at 1 and all other readings for the  
210 sample set calculated relative to this value.

211

#### 212 Construction of lentiviral vectors and transduction of keratinocytes

213 Human KLK5 cDNA was cloned into the pCCL lentiviral vector containing upstream spleen focus-  
214 forming virus (SFFV) promoter and downstream enhanced green fluorescent protein (eGFP)  
215 reporter gene linked to KLK5 via an internal ribosomal entry sequence from the endomyocarditis  
216 virus. The vector encoding eGFP alone was used as negative control. Lentiviruses were produced  
217 by co-transfecting 293T cells. Infectious lentiviruses were harvested 48 and 72 hours post-  
218 transfection, and the culture supernatants were concentrated by ultracentrifugation. The lentivirus  
219 concentration were titrated by viral copy number using qPCR and flow cytometry and the titres of  
220 eGFP viral vector and KLK5/eGFP viral vector were  $8 \times 10^8$  and  $4 \times 10^8$  TU/ml, respectively.

221 Human primary keratinocytes and cell line Ntert were transduced by one round of exposure to  
222 eGFP or KLK5/eGFP vectors at an MOI of 10. Transduced cells were subcultured for further  
223 experiments.

224

#### 225 Intracellular calcium mobilization assay

226 Measurement of intracellular calcium mobilization was performed using FluoForte Calcium Assay  
227 kit (Enzo Life Sciences, Exeter, UK). Mobilization of intracellular calcium was detected utilizing a  
228 fluorogenic calcium-binding dye. Keratinocytes were plated in 96-well plates at the density of  $1 \times$   
229  $10^4$  cells per well. After 24 hours, the growth medium was removed and 100 $\mu$ l of dye-loading  
230 solution was added. The cells were further incubated with the dye-loading solution for 45 min at  
231 37°C and then 15 minutes at room temperature. The cells were then inoculated with 100  $\mu$ M of  
232 PAR2 activating peptide SLIGKV-NH<sub>2</sub>, (Bachem, Cambridge Bioscience, Cambridge, UK), and

233 intracellular calcium signal was recorded via real-time monitoring of fluorescence intensity at  
234 excitation of 530 nm and emission of 570 nm using the microplate reader FLUOstar OPTIMA,  
235 (BMG, Lutterworth, UK). Intracellular calcium mobilization was calculated as changes of  
236 fluorescence intensity in relative fluorescence units (RFU) and the mobilisation curves were  
237 generated by RFU values plotted against the time.

238

#### 239 Western blotting

240 Cells were suspended in a cooled lysis buffer composed of 50 mM Tris-HCl pH 8.0, 150 mM NaCl,  
241 5 mM EDTA, cocktail protease inhibitors and 1 mM PMSF. Samples were incubated for 15 minutes  
242 at 4°C and then were centrifuged at 12,000 RPM for 15 minutes. The total protein concentration in  
243 the supernatant of lysed sample was determined by Bio-Rad protein assay Kit (Bio-Rad,  
244 Hertfordshire, UK). Samples were further diluted 5 times in 0.5 mM Tris-HCl pH 6.8 sample buffer  
245 containing 100 mM DTT, 10% SDS, 30% glycerol, 0.001% bromphenol blue. Equal amounts of  
246 total protein were loaded in SDS-PAGE. After electrophoresis, proteins were transferred to PVDF  
247 membranes and incubated with primary antibody overnight. The following day, membranes were  
248 incubated with secondary antibody conjugated with horseradish peroxidase (Sigma, Poole, UK),  
249 and signals were detected using the ECL Prime system (GE Healthcare, Bucks, UK). Ponceau red  
250 (Sigma-Aldrich, Poole, UK) staining was used as loading control for culture supernatants.

251

#### 252 In situ zymography and casein gel zymography

253 *In situ* zymography assay using casein-derived substrate measured the total protease activity in the  
254 skin. Briefly, the frozen skin sections were rinsed with PBS containing 0.1% Triton X-100 (Sigma-  
255 Aldrich, Poole, UK) and incubated at 37°C with 10 µg/ml casein conjugated with BODIPY TR-X  
256 (Life Technologies, Paisley, UK) in the buffer containing 10 mM Tris-HCl, pH7.8 in a humid  
257 chamber for two hours,. The fluorescent intensity was detected under a fluorescence microscope  
258 and quantified using Image-Pro.

259 Casein gel zymography was used for cells that were cultured in keratinocyte culture media without  
260 FCS for 48 hours. The culture media were then collected and concentrated using Amicon  
261 centrifugal filter devices (Millipore, Watford, UK). Samples were re-dissolved in non-reducing  
262 Novex® Tris-Glycine SDS sample buffer (Life Technologies, Paisley, UK) and separated on 12%  
263 polyacrylamide gels copolymerized with casein substrate (Life Technologies, Paisley, UK). After  
264 electrophoresis, the gels were soaked in renaturing buffer containing 50 mM Tris, pH 8 and 2.5%  
265 Triton X-100 for 1 hour. The gels were then incubated in developing buffer containing 50 mM Tris,  
266 pH 8 (Life Technologies, Paisley, UK) at 37°C overnight. Casein degrading activity was visualized  
267 when the gels were stained with 1% Coomassie Brilliant blue (Sigma-Aldrich, Poole, UK).

268

#### 269 Human cytokine antibody array

270 The cytokines in culture media collected from the different cell lines were assessed using The  
271 Human Cytokine Antibody Array Panel A kit (R&D System, Oxfordshire, UK) according to the  
272 manufactory's instruction. A total number of 36 cytokines were measured and the intensities of the  
273 blots were quantified by densitometry. As each reference or target protein was blotted in duplicate,  
274 mean pixel density from duplicate blots was calculated and normalised by reference blots.

275

#### 276 RT-PCR for IL-8

277 Following RNA extraction using the RNeasy® Plus Mini Kit (Qiagen), a second genomic DNA  
278 elimination step was employed to prevent genomic DNA contamination, and cDNA was then  
279 synthesised using the RT<sup>2</sup> first strand kit (SABioScience). Quantitative PCR was performed in  
280 duplicate wells for each time point using a 7900HT Fast Real-Time PCR System (Applied  
281 Biosystems, CA, USA) and the data collected using SDS 2.4 software (Applied Biosystems, CA,  
282 USA). The PCR protocol consisted of an initial cDNA denaturation at 95°C for 10 min, followed  
283 by 35 cycles of denaturation at 95°C for 15 seconds and annealing and data collection at 60°C for  
284 60 seconds.  $\Delta$ CT values were calculated using the Ct value for the housekeeping gene 26S and

285 analysis of fold change in gene regulation was performed using automated Microsoft Excel analysis  
286 tools from SABioscience.

287

#### 288 Enzyme linked immunosorbent assay (ELISA)

289 Cells were seeded in 24 well plates and cultured until confluence, then cultured in serum free media  
290 for 48 hours before culture media were collected and concentrated using Amicon centrifugal filter  
291 devices (Millipore, Watford, UK). The total protein concentration was quantified using Bio-Rad  
292 protein assay kit. The level of IL-8 was measured using IL-8 ELISA kit (BD Biosciences, Oxford,  
293 UK). TSLP and IL-10 were quantified using ELISA kits from eBioscience (eBioscience, Hatfield,  
294 UK). All sample reads were normalized to the total protein concentration.

295

#### 296 Bio-engineered skin sheet and grafting onto immunodeficient mice

297 The methods of generating bio-engineered skin sheet and grafting to mice were as described by Di  
298 et al<sup>19</sup>. Briefly, primary human keratinocytes were seeded on the top of a fibrin matrix populated  
299 with primary human fibroblasts. After keratinocytes reached confluence, the bioengineered skin  
300 constructs were grafted onto the dorsum of 6 weeks old female immunodeficient mice (NMRI  
301 strain, Charles River, UK). 8 weeks after grafting, skin samples from grafts were taken post-mortem  
302 and formalin fixed and paraffin-embedded or OCT-embedded. H&E staining and immunostaining  
303 for KLK5, FLG and DSG1, and zymographics were performed on these tissues.

304

305

306

307

308

309

## 310 **Results**

### 311 **Increased expression and activity of KLK5 in AD skin**

312 Skin biopsies taken from lesional and non-lesional skin in five children with AD were examined for  
313 epidermal morphology and KLK5 expression. Five age-matched normal donor skin biopsies were  
314 used as controls. Compared to normal skin, AD lesional skin exhibited epidermal changes including  
315 acanthosis, spongiosis, parakeratosis and elongated rete ridges. Non-lesional skin also showed  
316 histopathological characteristics consistent with the disease, but far less prominent than those  
317 observed in lesional skin (**Figure 1A. a-c**). The expression of KLK5, as detected by  
318 immunostaining, was localised in the cornified layer in normal skin, whereas in AD skin, especially  
319 in the lesional skin, KLK5 was present in the granular layer and upper stratum spinosum with high  
320 staining intensity (**Figure 1A. d-f and Supplementary materials, Figure S1**). Quantification of  
321 KLK5 based on mean optical staining intensity/area further demonstrated significant increased  
322 expression of KLK5 in both lesional and non-lesional AD skin, compared to the normal skin  
323 ( $p < 0.05$ ) (**Figure 1B**). As DSG1 is the proteolytic substrate of KLK5, and FLG can be degraded by  
324 elastase 2 which is a serine protease activated by KLK5 in the skin<sup>20</sup>, DSG1 and FLG expressions  
325 were also examined by immunostaining. Both FLG and DSG1 expression were significantly  
326 reduced in lesional skin of AD ( $p < 0.05$ ) (**Figure 1A. g-i & j-l, Figure 1B**). The protease activity in  
327 the skin were further examined by *in situ* staining, and results showed a similar location and  
328 staining pattern to KLK5 expression with more diffuse and enhanced fluorescence intensity in the  
329 AD skin (**Figure 1A. m-o, Figure 1B and Supplementary materials, Figure S2**). Although the  
330 caseinolytic serine protease assay detects total protease activity, as KLK5 is a major serine protease  
331 in the skin<sup>2</sup> and the protease activity closely matched the extent and distribution of KLK5 protein  
332 expression, it is likely that KLK5 is a significant contributor to the increased activity of serine  
333 protease observed in the AD skin.

334

335 **Transient up-regulation of KLK5 stimulated PAR2, but persistent activated KLK5**  
336 **desensitised PAR2**

337 The expression of the KLK5 targeted molecule PAR2 was further examined in the donor skin (n=5)  
338 and AD non-lesional and lesional skin by immunostaining. No significant changes in PAR2  
339 expression was noted in lesional, non-lesional AD skin and normal donor skin ( $p>0.05$ ) (**Figure 1A.**  
340 **p-r, Figure 1B**), although there was a fluctuation of PAR2 expression level among individuals.  
341 This result suggests that up-regulated KLK5 does not modify PAR2 in AD skin. Considering that  
342 the up-regulation of KLK5 was likely to be chronic and persistent in AD skin, we speculated that  
343 the response of PAR2 to KLK5 might differ between AD skin and skin with transient KLK5 up-  
344 regulation. To determine this, the influence of transiently increased KLK5 on PAR2 was tested  
345 using an *ex-vivo* irritant dermatological model in which irritants were applied onto normal skin  
346 cultured *in vitro*. Following the application of croton oil or SDS or acetone for 30 minutes on the  
347 *ex-vivo* skin model, increased epidermal expression of KLK5 and PAR2 were detected in the  
348 epidermis (**Figure 2. a**). Quantification using image analysis confirmed significantly higher  
349 expression of both KLK5 and PAR2 across all layers of the epidermis (**Figure 2. b-e**).

350 The effect of persistently increased KLK5 on PAR2 was tested in the keratinocyte cell line Ntert  
351 (KLK5-Ntert) or primary keratinocytes (KLK5-pKC) ectopically over-expressing KLK5. Cells  
352 transduced with eGFP vector alone were used as control (GFP-Ntert or GFP-pKC). The  
353 transduction efficiency in both KLK5 transduced cells and GFP transduced cells was nearly 60% as  
354 determined by eGFP expression. Overexpression of KLK5 in KLK5-transduced cells and culture  
355 media was confirmed by western blotting (**Figure 3. a&c**). The activity of KLK5 was further  
356 assessed by zymography. Active KLK5 was detected in the culture media collected from KLK5  
357 transduced cell culture (**Figure 3. d**), but not in cell lysates (**Figure3. b**). KLK5 is synthesized as  
358 inactive pre-pro-KLK5 (precursor or zymogene) which is then translocated into the endoplasmic  
359 reticulum in cells (see review by Debela M *et al*)<sup>21</sup>. Following the removal of the signal peptide  
360 (~30 amino acids), the pre-pro-KLK5 becomes pro-KLK5 that is secreted into the extracellular

361 space and subsequently becomes activated upon release of its 37 amino acids propeptide from the  
362 N-terminus of KLK5. Thus, the KLK5 extracted from the cells would not contain the final activated  
363 KLK5 and it is not surprising that there was no positive digested band detected in zymography  
364 loaded with cell lysates. In contrast, a digested band was seen in zymography loaded with culture  
365 medium from cells over expressing KLK5/eGFP as a result of the culture medium containing the  
366 active form of KLK5. Although a ~70kDa band was present on both western blotting and  
367 zymography, the intensity of the protein band remained unchanged among cell lysates from  
368 untransduced cells, cells transduced with GFP alone and KLK5/GFP, therefore this was considered  
369 to represent a nonspecific protein, but having a proteolytic activity on casein-derived substrate.

370 The durability of KLK5 expression in both KLK5-Ntert and KLK5-pKC was assessed following  
371 propagation of transduced cells and there was no decline in KLK5 expression over this time as  
372 determined by eGFP expression, indicating persistent KLK5 expression in the KLK5-cell model  
373 (**Supplementary materials, Figure S3**). As a previous study showed that PAR2 was mainly  
374 expressed in differentiated keratinocytes, the Ntert cell line was checked for differentiation markers  
375 keratin 10 and involucrin and results showed positive expression for both proteins (**Supplementary**  
376 **materials, Figure S4**). The activity of PAR2 and a KLK5 down-stream target was then examined  
377 in untransfected Ntert (UT-Ntert), GFP-Ntert and KLK5-Ntert by a PAR2-dependent calcium  
378 mobilisation assay. Mobilisation of calcium was observed in the untransfected keratinocytes after  
379 addition of a PAR2 agonist (AP), and similarly following addition of recombinant KLK5 (rKLK5),  
380 albeit slightly later than that induced by AP (**Figure 4. a**), confirming that KLK5 was able to  
381 activate PAR2. In contrast, a decline in calcium mobilisation was detected in KLK5-Ntert cells  
382 compared to that in GFP-Ntert (**Figure 4. b**). Thus, a different PAR2 dependent calcium  
383 mobilisation response was observed in cells with persistent expression of KLK5 versus cells with  
384 transient rKLK5 stimulation.

385 PAR2, like many other receptors, can be desensitized if continuously or repeatedly exposed to its  
386 agonist<sup>22,23</sup>, and these results suggest that persistent over-expression of KLK5 could desensitise the

387 PAR2 receptor resulting in a lower response of PAR2 to its agonist AP. Since PAR2 desensitisation  
388 can be reversed by removal of PAR2 activators, we looked at calcium mobilisation when KLK5-  
389 Ntert cells were treated with the serine protease inhibitor SFTI-G, an analogue derived from the  
390 naturally occurring substance sunflower trypsin inhibitor 1<sup>24</sup>. Following treatment with 100µM  
391 SFTI-G overnight, the PAR2 dependent calcium mobilisation in KLK5-Ntert cells recovered to  
392 levels similar to that in GFP-Ntert and untransfected keratinocytes (**Figure 4. c**).

393

### 394 **Persistently activated KLK5 induced cytokine expression/secretion despite PAR2** 395 **desensitisation**

396 Activated PAR2 induced pro-inflammatory cytokine elevation and secretion, including of IL-8, has  
397 been reported<sup>25</sup>. In the *ex-vivo* irritant dermatological skin model, increased IL-8 mRNA expression  
398 was detected by RT-PCR within 12 hours following exposure to SDS and to a lesser extent at 12  
399 hours following application of croton oil (**Figure 5. a**). In the KLK5-pKC cells with persistent  
400 KLK5 expression, IL-8 protein, measured by cytokine antibody array, was also increased (**Figure**  
401 **5.b&c**). In addition, IL-10 was elevated in KLK5-pKC cells (**Figure 5. b&c**), but other cytokines  
402 including IL-1, IL-4, IL-6 and IFN-gamma were not (**Supplementary materials, Table S1**). TSLP,  
403 a prominent pro-inflammatory cytokine in AD skin also showed increased expression in KLK5-  
404 pKC cells as measured by ELISA (**Figure 5. c**). However, increased IL-10 and TSLP were not  
405 detected in cells transiently challenged with rKLK5 (data not shown).

406

### 407 **Inhibition of persistent KLK5 activity reversed KLK5 effects on DSG1 and cytokine** 408 **production**

409 To examine the downstream effects of inhibition of persistently raised KLK5 activity, primary  
410 keratinocytes transduced with KLK5 (KLK5-pKC) or eGFP (GFP-pKC) were cultured in serum  
411 free media inoculated with 100 µM of serine protease inhibitor SFTI-G for twenty-four hours.  
412 Although the level of secreted KLK5 in culture media, as determined by western blot, remained



413 elevated in the KLK5-pKC cells 24 hours post SFTI-G treatment, the expression of full length  
414 DSG1 was restored in treated KLK5-cells compared to untreated cells, whereas there was no  
415 significant change in the level of DSG1 in GFP-pKC cells before (-) and after SFTI-G (+)  
416 treatment, indicating the suppression of KLK5 activity by SFTI-G in the KLK-5 culture (**Figure 6.**  
417 **a**). It was noticed that in KLK5-pKC cells, there was no DSG1 detected. The DSG1 antibody used  
418 in the study was a monoclonal antibody (clone P124) recognizing the N-terminal extracellular  
419 domain of DSG1 and full length DSG1. Primary keratinocytes were used for untreated as well as  
420 treated experiments, and treated cells showed a DSG1 band. Therefore, no DSG1 band in KLK5-  
421 pKC cells without SFTI-G treatment was most likely due to DSG1 levels being too low to be  
422 detected and/or the antibody does not recognize the cytoplasm domain of DSG1 alone following the  
423 cleavage of the extracellular domain by over-expressed/activated KLK5. Cytokines IL-8, IL-10 and  
424 TSLP were also significantly reduced in SFTI-G treated KLK5-pKC cells, compared to untreated  
425 KLK5-pKC cells, and these changes were not observed in treated or untreated GFP-cells as  
426 confirmed by both cytokine antibody array and ELISA (**Figure 5.b, 6.b&c, Supplementary**  
427 **materials, Table S1**).

428

#### 429 **Keratinocytes with persistent activated KLK5 exhibit an AD-like epidermal architecture**

430 To examine the influence of persistently up-regulated KLK5 activity on epidermal architecture *in*  
431 *vivo*, primary keratinocytes from the non-lesional skin in a patient with AD (AD-pKC), or primary  
432 normal keratinocytes ectopically over-expressing KLK5 (KLK5-pKC) or GFP (GFP-pKC) were  
433 cultured *in vitro* as bio-engineered skin and grafted onto immuno-deficient mice. 8 weeks post-  
434 grafting, the skin from the grafted area was harvested. Grafts generated from KLK5-pKCs and AD-  
435 pKC showed AD-like morphology, with acanthosis, mild parakeratosis and enlarged intercellular  
436 spaces compared to the GFP-pKC graft (**Figure 7. a-c**). Increased expression of KLK5 and protease  
437 activity and decreased DSG1 were observed in both KLK5-pKC and AD-pKC grafts compared to  
438 GFP-cell graft (**Figure 7. d-l**), which were analogous to findings in AD skin. Altered FLG

439 expression was also detected in KLK5-pKC and AD-pKC grafts, it was more evident in the upper  
440 stratum spinosum similar to that seen in the AD skin (**Figure 7. m-o and Figure 1A. h&i**). As the  
441 FLG antibody used for the study only detects FLG produced from human cells, the mouse-human  
442 skin boundary was easily visible in the FLG stained skin, indicating that the keratinocytes within  
443 the grafts were of human origin (**Figure 7. g-i**). In addition, the mouse-human skin boundary  
444 images showed an increased thickness of mouse epidermis (acanthosis) next to the grafts generated  
445 by KLK5-pKC and AD-pKC, but not by the GFP-pKC, which may have resulted from a paracrine  
446 effect of activated KLK5 secreted from these grafts.

447

448

449

450

451

452

453

454

455

456

457

458

459

460

461

462

## 463 **Discussion**

464 Up regulated KLK5 together with skin barrier defects in AD has been reported in previous  
465 studies<sup>10,11,26</sup>, which have shown that both genetic and environmental factors can cause aberrant  
466 KLK5 activity. Indeed, as AD shares a number of clinical features with NS, it has been speculated  
467 that AD might also share some pathological mechanisms of dysfunctional skin barrier with NS<sup>27,28</sup>.  
468 Genome-wide association studies have shown several single nucleotide polymorphisms (SNPs) in  
469 *SPINK5* associated with AD, in particular Glu420Lys<sup>28</sup> and functional investigations have further  
470 confirmed that Glu420Lys SNP alters *SPINK5* encoded protein LEKTI proteolytic activation and  
471 results in dysregulation of proteases including the KLKs<sup>29</sup>. Environmental factors that disrupt the  
472 skin barrier, including irritants and infection, and trigger KLK5 up-regulation have also been  
473 reported<sup>30</sup>. In this study, we have demonstrated that the irritants croton oil and SDS increase KLK5  
474 and PAR2 expression, but that transient KLK5 expression seems to have different effects on PAR2  
475 expression/activity than that observed with persistent KLK5 expression.

476 KLK5 activation of PAR2 has been demonstrated previously<sup>31</sup> and we also showed rKLK5  
477 activated PAR2 in this study using an intracellular calcium mobilization fluorescence assay. The  
478 fluorescence peak induced by rKLK5 was, however, delayed 40-50 seconds compared to the peak  
479 induced by the PAR2 agonist (AP). This difference in peak time was likely to be due to the tethered  
480 ligand mechanism with regards to maximum rate of PAR2 activation by KLK5. Oikonomopoulou  
481 and colleagues<sup>31</sup> have reported that KLK5 activation of PAR2 is a two-step process involving  
482 cleavage and tethered ligand binding to the PAR2 receptor, whereas a one-step process is involved  
483 in the PAR2 agonist directly binding to the receptor.

484 The signalling pathway of KLK5-PAR2-NFκB-cytokines has been recognised for more than a  
485 decade<sup>32,33</sup>, but most studies have been carried out in models with transient exposure to exogenous  
486 rKLK5<sup>31</sup>. PAR2 can exhibit desensitization due to continuous or repeated stimulation by its agonist,  
487 leading to reduced responsiveness<sup>34</sup>. AD is a chronic skin condition, and up-regulated KLK5  
488 activity in affected skin is most likely to be persistent than transient. However, the examination of

489 PAR2 activity in skin *in situ* is technically difficult. Currently, the activity of PAR2 is assessed by  
490 intra-cellular calcium mobilization in live cells following stimulation/inhibition with its  
491 agonist/antagonist. Tissues from AD skin or murine AD models are generally fixed/embedded or  
492 snap frozen, and thus are not suitable for use in the calcium mobilization assay. There is an indirect  
493 way to check PAR2 activity by examination of PAR receptor internalization, e.g. by tracking GFP-  
494 tagged PAR2 fusion protein trafficking<sup>35</sup> or by analysing the distribution of activated (cytoplasmic)  
495 and unactivated (cell membrane) PAR2 receptor<sup>36</sup>, but these also require cell-culture models rather  
496 than skin tissue. However, although the desensitisation of PAR2 in the skin *in situ* cannot be  
497 measured directly, previous work by Moniaga and colleagues<sup>37</sup> supports our view that PAR2 is  
498 desensitised in AD-like skin lesions. In their study<sup>37</sup>, a PAR2 agonist could up-regulate TLSP in  
499 murine keratinocytes following transient (one-off) stimulation, but only a marginal increase of  
500 TSLP production was noted in the skin of flaky tail mice following repeated topical application of  
501 dust mite for 7 weeks; this discrepancy of TLSP production between transient stimulation in cell  
502 culture and repeated challenge in mouse skin was probably because the repeated challenge caused  
503 PAR2 desensitisation, resulting in low PAR2 activity. Related to this, an *in vivo* study by Briot and  
504 colleagues showed that TLSP production was independent of PAR2 activation and that PAR2 was  
505 not central to the production of the skin inflammation when there was persistent KLK5 activity<sup>38</sup>.  
506 In mice with double knockout of SPINK5<sup>-/-</sup> and PAR2<sup>-/-</sup> and high KLK activity, the deletion of  
507 PAR2 in the adult double knockout-grafted skin did not result in the reduction of TLSP and did not  
508 suppress the skin inflammation<sup>38</sup>. This result suggests that the inflammatory skin in Netherton  
509 syndrome and AD is not solely caused by PAR2 activation.

510 Based on our observations in the AD skin with persistent KLK5 overexpression and the *ex-vivo*  
511 irritant dermatological skin model mimicking a transiently increased KLK, we demonstrated that  
512 PAR2 had a higher response to transient KLK5 stimulation, but had a weak response to persistent  
513 KLK5 stimulation. Interestingly, despite the low activity of PAR2 in cells overexpressing KLK5,  
514 these cells up-regulated and secreted pro-inflammatory and Th2-polarizing cytokines, including IL-

515 8, IL-10 and TSLP, indicating that persistent KLK5 induced IL-8, IL-10 and TSLP. The exact  
516 pathway of persistent KLK5 expression/activity induced IL8, IL10 and TLSP secretion in KLK5-  
517 pKC remains unclear, and further investigations will be required to elucidate this. The keratinocyte-  
518 based nature of our KLK5 over-expressing model, which lacks immune cells, meant that it was not  
519 possible to investigate cytokine secretion from immune cells following KLK5 activation, which  
520 may explain why our cytokine antibody array data did not show elevation of other  
521 cytokines/chemokines reported in AD patients (such as IL-6, IL-4, GM-CSF, IL-1 and TNF $\alpha$ ).

522 The influence of activated KLK5 on epidermal architecture in the *in vivo* human: murine chimeric  
523 skin graft model, which showed AD-like skin architecture in grafts generated using cells over-  
524 expressing KLK5, further indicated that KLK5 plays a key role in this process. Similar observations  
525 have also been detected using a transgenic mouse model over-expressing KLK5<sup>39</sup>. Furthermore, as  
526 the human: murine chimeric skin graft model was immunodeficient and maintained in specific  
527 pathogen-free environment, our results suggest that the AD-like histopathological features and  
528 abnormal barrier protein expression in the epidermis generated by AD-cells and KLK5-pKC cells  
529 were a specific consequence of persistent up-regulation of KLK5 in the keratinocytes.

530 Our study also suggests that increased KLK5 in AD skin should not simply be viewed as a  
531 ‘biomarker’ in this skin disorder, but as a protease which has significant functional impact in this  
532 condition. In AD patients, environmental factors can trigger the cytokine cascade and stimulate a  
533 Th2-skewed inflammatory infiltrate through the initial defective skin barrier, resulting in  
534 susceptibility to allergy or ‘atopy’ (“outside-inside” aetiological mechanism)<sup>16,40</sup>. The induced  
535 inflammatory response further compromises barrier function, causing keratinocyte damage and  
536 inducing upregulation of certain molecules, such as KLK5. The initial damage secondary to  
537 increased KLK5 forms a vicious cycle of inflammation-induced barrier impairment in AD (outside-  
538 inside-outside)<sup>16</sup>.

539 Amongst the currently known inhibitors of kallikreins<sup>41-43</sup>, the naturally occurring cyclic peptide  
540 SFTI has been extensively investigated due to it being amenable to chemical manipulation which

541 has allowed for the creation of synthetic variants<sup>44-46</sup>. We used the analogue SFTI-G derived from  
542 SFTI<sup>24</sup> to control KLK5 activity and our *in vitro* results showed a normalised DSG1 expression,  
543 depletion of depressed PAR2 dependent calcium mobilisation and reduction of IL-8, IL-10 and  
544 TSLP. Thus, reducing KLK5 activity could offer a therapeutic option for the treatment of AD,  
545 where control of higher KLK5 activity might help to reverse (at least part of) the AD phenotype in  
546 patients with this disorder.

547

## 548 **Acknowledgements**

549 The authors are grateful to David Rew, University Hospital Southampton NHS Foundation Trust  
550 for assistance in procuring skin samples.

551

552

553

554

555

556

557

558

559 **Legends**

560 **Figure 1. Skin morphology and protein expression in AD**

561 A: Skin sections from normal donor (n=5) and AD skin (n=5) were examined by H&E (a-c),  
562 immunostaining (d-l & p-r), and *in situ* zymography (m-o). Green/brown colour represents protein  
563 expression or protease activity. Nuclei were stained in blue colour. Scale bar = 50 µm.

564 B: Quantification of staining intensity (n=3 per sample) was measured by mean staining  
565 intensity/area using ImagePro.

566

567 **Figure 2. Increased KLK5 and PAR2 expression in *ex-vivo* dermatitis skin model**

568 Immunofluorescence staining of epidermal KLK5 and PAR2 following application of 3% croton oil  
569 and 5% SDS compared with acetone-treated and PBS-treated skin. Quantification of relative KLK5  
570 (b,d) and PAR2 (c,e) expression from stratum corneum to basal layer (0%-100% depth  
571 respectively). KLK5 (n=9, n=7), PAR2 (n=7, n=6) for 3% croton oil and 5% SDS respectively.

572

573 **Figure 3. Characterisation of keratinocyte over expressing KLK5**

574 The expression and activity of KLK5 in cell lysate (a,b) and culture media (c,d) from the cells  
575 transfected with KLK5 gene were examined by Western blot (left panel) and gel zymography (right  
576 panel). β-actin were used as loading controls. UT = untransduced cells; eGFP = cells transduced  
577 with eGFP alone vector; KLK5 = cells transduced with KLK5/eGFP vector and rKLK = activated  
578 recombinant KLK5 protein (where rKLK was added directly to the gel as a positive zymography  
579 control).

580

581 **Figure 4. PAR2-dependent calcium mobilisation in keratinocytes**

582 PAR2-dependent calcium mobilisation was measured in untransfected Ntert cells challenged with  
583 AP or rKLK5 (a); cells transfected with GFP or KLK5 challenged with AP (b); and cells transfected

584 with GFP or KLK5, treated with SFTI-G and then challenged with AP (c). PBS was used as  
585 negative control.

586

587 **Figure 5. Cytokine expression in keratinocytes**

588 Cytokine levels were measured in the *ex-vivo* skin model with transiently up-regulated KLK5 using  
589 RT-PCR for IL8 (a); KLK5-pKC cells with persistent KLK5 expression using antibody array blots  
590 (b). The IL-8 and IL-10 levels detected by cytokine antibody array and quantified by mean pixel  
591 density, and TSLP level measured by ELISA are shown in the bar chart (c). Data in (a) are shown  
592 relative to PBS-treated skin.

593

594 **Figure 6. The inhibition of KLK5 by serine protease inhibitor SFTI-G**

595 Primary keratinocytes transduced with GFP or KLK5 gene were treated with 100µM of SFTI-G  
596 overnight. KLK5 in culture media and DSG1 in cell lysates were measured by Western blot (a).  
597 Cytokine secretions in the culture media following SFTI-G treatment were measured by cytokine  
598 antibody array (b) and confirmed by ELISA (c). The symbol \* is representative of statistical  
599 significance ( $p < 0.05$ ) and NS stands for non-significance.

600

601 **Figure 7. Persistent KLK5 activity induced AD-like skin changes**

602 A: Skin graft sections from human: murine skin graft mice were examined for morphology by H&E  
603 (a-c), KLK5 (d-f) expression by immunohistochemistry, DSG1 (j-l) and FLG (m-o) expression by  
604 immunofluorescence, and protease activity (g-i) by *in situ* zymography. Brown and green colour  
605 show protein expression/protease activity and purple and blue colour show stained nuclei. Scale  
606 Bar= 50 µm.



## References

1. Lundwall A and Brattsand M, Kallikrein-related peptidases, *Cell Mol Life Sci*, 2008 Jul, 65(13):2019-2038.
2. Brattsand M et al., A proteolytic cascade of kallikreins in the stratum corneum, *J Invest Dermatol*, 2005 Jan, 124(1):198-203.
3. Sales KU et al., Matriptase initiates activation of epidermal pro-kallikrein and disease onset in a mouse model of Netherton syndrome, *Nat Genet*, 2010 Aug, 42(8):676-683.
4. Caubet C et al., Degradation of corneodesmosome proteins by two serine proteases of the kallikrein family, SCTE/KLK5/hK5 and SCCE/KLK7/hK7, *J Invest Dermatol*, 2004 May, 122(5):1235-1244.
5. Chavanas S et al., Mutations in SPINK5, encoding a serine protease inhibitor, cause Netherton syndrome, *Nat Genet*, 2000 Jun, 25(2):141-142.
6. Descargues P et al., Corneodesmosomal cadherins are preferential targets of stratum corneum trypsin- and chymotrypsin-like hyperactivity in Netherton syndrome, *J Invest Dermatol*, 2006 Jul, 126(7):1622-1632.
7. Stefansson K et al., Kallikrein-related peptidase 14 may be a major contributor to trypsin-like proteolytic activity in human stratum corneum, *Biol Chem*, 2006 Jun, 387(6):761-768.
8. Steinhoff M et al., Proteinase-activated receptors: transducers of proteinase-mediated signaling in inflammation and immune response, *Endocr Rev*, 2005 Feb, 26(1):1-43.
9. Yamasaki K et al., Kallikrein-mediated proteolysis regulates the antimicrobial effects of cathelicidins in skin, *FASEB J*, 2006 Oct, 20(12):2068-2080.
10. Komatsu N et al., Human tissue kallikrein expression in the stratum corneum and serum of atopic dermatitis patients, *Exp Dermatol*, 2007 Jun, 16(6):513-519.
11. Voegeli R et al., Increased stratum corneum serine protease activity in acute eczematous atopic skin, *Br J Dermatol*, 2009 Jul, 161(1):70-77.
12. Angelova-Fischer I, Irritants and Skin Barrier Function, *Curr Probl Dermatol*, 2016, 49:80-89.
13. Palmer CN et al., Common loss-of-function variants of the epidermal barrier protein filaggrin are a major predisposing factor for atopic dermatitis, *Nat Genet*, 2006 Apr, 38(4):441-446.
14. Vasilopoulos Y et al., Genetic association between an AACC insertion in the 3'UTR of the stratum corneum chymotryptic enzyme gene and atopic dermatitis, *J Invest Dermatol*, 2004 Jul, 123(1):62-66.
15. Walley AJ et al., Linkage and allelic association of chromosome 5 cytokine cluster genetic markers with atopy and asthma associated traits, *Genomics*, 2001 Feb, 72(1):15-20.
16. Elias PM and Schmuth M, Abnormal skin barrier in the etiopathogenesis of atopic dermatitis, *Curr Allergy Asthma Rep*, 2009 Jul, 9(4):265-272.

17. Di WL et al., Human Involucrin Promoter Mediates Repression-Resistant and Compartment-Specific LEKTI Expression, *Hum Gene Ther*, 2012 Jan, 23(1):83-90.
18. Dickson MA et al., Human keratinocytes that express hTERT and also bypass a p16(INK4a)-enforced mechanism that limits life span become immortal yet retain normal growth and differentiation characteristics, *Mol Cell Biol*, 2000 Feb, 20(4):1436-1447.
19. Di WL et al., Ex-vivo gene therapy restores LEKTI activity and corrects the architecture of Netherton syndrome-derived skin grafts, *Mol Ther*, 2011 Feb, 19(2):408-416.
20. Bonnart C et al., Elastase 2 is expressed in human and mouse epidermis and impairs skin barrier function in Netherton syndrome through filaggrin and lipid misprocessing, *J Clin Invest*, 2010 Mar, 120(3):871-882.
21. Debela M et al., Structures and specificity of the human kallikrein-related peptidases KLK 4, 5, 6, and 7, *Biol Chem*, 2008 Jun, 389(6):623-632.
22. Bohm SK et al., Mechanisms of desensitization and resensitization of proteinase-activated receptor-2, *J Biol Chem*, 1996 Sep, 271(36):22003-22016.
23. Stefansson K et al., Activation of proteinase-activated receptor-2 by human kallikrein-related peptidases, *J Invest Dermatol*, 2008 Jan, 128(1):18-25.
24. Shariff L et al., Sunflower trypsin inhibitor (SFTI-1) analogues of synthetic and biological origin via N-S acyl transfer: potential inhibitors of human Kallikrein-5 (KLK5), *Tetrahedron*, 2014, 70:7675-7680.
25. Hou L et al., Immunolocalization of protease-activated receptor-2 in skin: receptor activation stimulates interleukin-8 secretion by keratinocytes in vitro, *Immunology*, 1998 Jul, 94(3):356-362.
26. Komatsu N et al., Multiple tissue kallikrein mRNA and protein expression in normal skin and skin diseases, *Br J Dermatol*, 2005 Aug, 153(2):274-281.
27. Di WL et al., A heterozygous null mutation combined with the G1258A polymorphism of SPINK5 causes impaired LEKTI function and abnormal expression of skin barrier proteins, *Br J Dermatol*, 2009 Aug, 161(2):404-412.
28. Walley AJ et al., Gene polymorphism in Netherton and common atopic disease, *Nat Genet*, 2001 Oct, 29(2):175-178.
29. Fortugno P et al., The 420K LEKTI variant alters LEKTI proteolytic activation and results in protease deregulation: implications for atopic dermatitis, *Hum Mol Genet*, 2012 Oct, 21(19):4187-4200.
30. Torma H, Lindberg M, and Berne B, Skin barrier disruption by sodium lauryl sulfate-exposure alters the expressions of involucrin, transglutaminase 1, profilaggrin, and kallikreins during the repair phase in human skin in vivo, *J Invest Dermatol*, 2008 May, 128(5):1212-1219.
31. Oikonomopoulou K et al., Kallikrein-mediated cell signalling: targeting proteinase-activated receptors (PARs), *Biol Chem*, 2006 Jun, 387(6):817-824.

32. Rallabhandi P et al., Analysis of proteinase-activated receptor 2 and TLR4 signal transduction: a novel paradigm for receptor cooperativity, *J Biol Chem*, 2008 Sep, 283(36):24314-24325.
33. Buddenkotte J et al., Agonists of proteinase-activated receptor-2 stimulate upregulation of intercellular cell adhesion molecule-1 in primary human keratinocytes via activation of NF-kappa B, *J Invest Dermatol*, 2005 Jan, 124(1):38-45.
34. Soh UJ et al., Signal transduction by protease-activated receptors, *Br J Pharmacol*, 2010 May, 160(2):191-203.
35. Ramsay AJ et al., Kallikrein-related peptidase 4 (KLK4) initiates intracellular signaling via protease-activated receptors (PARs). KLK4 and PAR-2 are co-expressed during prostate cancer progression, *J Biol Chem*, 2008 May, 283(18):12293-12304.
36. Gratio V et al., Kallikrein-related peptidase 14 acts on proteinase-activated receptor 2 to induce signaling pathway in colon cancer cells, *Am J Pathol*, 2011 Nov, 179(5):2625-2636.
37. Moniaga CS et al., Protease activity enhances production of thymic stromal lymphopoietin and basophil accumulation in flaky tail mice, *Am J Pathol*, 2013 Mar, 182(3):841-851.
38. Briot A et al., Par2 inactivation inhibits early production of TSLP, but not cutaneous inflammation, in Netherton syndrome adult mouse model, *J Invest Dermatol*, 2010 Dec, 130(12):2736-2742.
39. Furio L et al., Transgenic kallikrein 5 mice reproduce major cutaneous and systemic hallmarks of Netherton syndrome, *J Exp Med*, 2014 Mar, 211(3):499-513.
40. Cork MJ et al., Epidermal barrier dysfunction in atopic dermatitis, *J Invest Dermatol*, 2009 Aug, 129(8):1892-1908.
41. Tan X et al., Toward the first class of suicide inhibitors of kallikreins involved in skin diseases, *J Med Chem*, 2015 Jan, 58(2):598-612.
42. Tan X et al., 1,2,4-Triazole derivatives as transient inactivators of kallikreins involved in skin diseases, *Bioorg Med Chem Lett*, 2013 Aug, 23(16):4547-4551.
43. Teixeira TS et al., Biological evaluation and docking studies of natural isocoumarins as inhibitors for human kallikrein 5 and 7, *Bioorg Med Chem Lett*, 2011 Oct, 21(20):6112-6115.
44. de Veer SJ et al., Mechanism-based selection of a potent kallikrein-related peptidase 7 inhibitor from a versatile library based on the sunflower trypsin inhibitor SFTI-1, *Biopolymers*, 2013 Sep, 100(5):510-518.
45. Swedberg JE et al., Substrate-guided design of a potent and selective kallikrein-related peptidase inhibitor for kallikrein 4, *Chem Biol*, 2009 Jun, 16(6):633-643.
46. de Veer SJ et al., Engineered protease inhibitors based on sunflower trypsin inhibitor-1 (SFTI-1) provide insights into the role of sequence and conformation in Laskowski mechanism inhibition, *Biochem J*, 2015 Jul, 469(2):243-253.

## Supplementary materials

**Table S1. Quantification of dots by densitometry for cytokine antibody array**

Coordinate of the plate	Target/control	Mean pixel density			
		GFP-pKC		KLK5-pKC	
		SFTI (-)	SFTI (+)	SFTI (-)	SFTI (+)
A1,A2	Reference spot	17896	17221	17701	17193
A3,A4	C5/C5a	232	294	245	302
A5,A6	CD40 ligand	216	259	241	226
A7,A8	G-CSF	308	299	327	302
A9,A10	GM-CSF	341	367	319	298
A11,A12	GRO-alpha	18958	19020	19110	19212
A13,A14	I-309	327	381	338	306
A15,A16	sICAM-1	404	394	420	441
A17,A18	IFN-gamma	336	385	312	397
A19,A20	Reference spot	16350	16361	16222	16119
B3,B4	IL-1a	188	226	209	198
B5,B6	IL-1b	217	275	232	202
B7,B8	IL-1ra	15933	15659	15899	16021
B9,B10	IL-2	297	310	268	289
B11,B12	IL-4	322	338	301	297
B13,B14	IL-5	275	311	291	298
B15,B16	IL-6	397	344	380	393
B17,B18	IL-8	15922	15273	22598	16276
C3,C4	IL-10	224	243	8236	268
C5,C6	IL-12 p70	313	289	326	301
C7,C8	IL-13	406	484	415	461
C9,C10	IL-16	359	331	360	314
C11,C12	IL-17	448	429	465	438
C13,C14	IL-17E	385	375	397	408
C15,C16	IL-23	535	521	519	569
C17,C18	IL-27	449	425	456	406

D3,D4	IL-32a	398	331	386	350
D5,D6	IP-10	421	452	409	398
D7,D8	ITAC	415	429	406	466
D9,D10	MCP-1	399	411	394	429
D11,D12	MIF	12868	12525	13310	12806
D13,D14	MIP-1a	275	310	298	322
D15,D16	MIP-1b	393	404	415	438
D17,D18	Serpin E1	18256	18010	18166	18125
E1,E2	Reference spot	17510	17725	17566	17621
E3,E4	RANTES	435	509	466	428
E5,E6	SDF-1	449	399	425	462
E7,E8	TNF-alpha	398	439	412	402
E9,E10	sTERM-1	421	461	435	489
E19,E20	Negative control	275	211	261	293

## Legends

### Figure S1. KLK5 expression in non-lesional and lesional skin from five AD patients

Skin sections from normal donor (n=5, control 1-5, left panel) and AD patients (n=5, patient 1-5) from non-lesional (middle panel) and lesional (right panel) skin were examined for KLK5 expression using immunohistochemistry. Brown colour represents protein expression and blue colour shows nuclei stain. Scale bar = 100  $\mu$ m.

### Figure S2. *In situ* protease activity in non-lesional and lesional skin from AD patients

Skin sections from normal donor (n=4, control 1-4, left panel) and AD patients (n=4, patient 1-4) from non-lesional (middle panel) and lesional (right panel) skin were examined for total protease activity by *in situ* zymography. Green colour represents protease activity, whereas nuclei are stained blue. Scale bar = 50  $\mu$ m.

### **Figure S3. Stability of transgene KLK5 expression in keratinocytes**

Primary keratinocytes and Ntert keratinocyte cell line were transduced with KLK5/eGFP transgene and the stability of transgene in cells was assessed by GFP positive cells (GFP+) using flow cytometry. Primary keratinocytes were only monitored for a period of 12 days due to proliferative lifespan of primary cells in *in vitro* culture.

### **Figure S4. Differentiation markers in Ntert keratinocytes**

Keratin 10 and involucrin expression in cell lysates from untransduced Ntert keratinocytes (UT), or transduced with KLK5 (KLK5) or eGFP vector alone (eGFP) were assayed by Western blot. Positive expressions of both proteins indicated a proportion of differentiated cells in the Ntert cell line.

Figure 1A  
[Click here to download high resolution image](#)

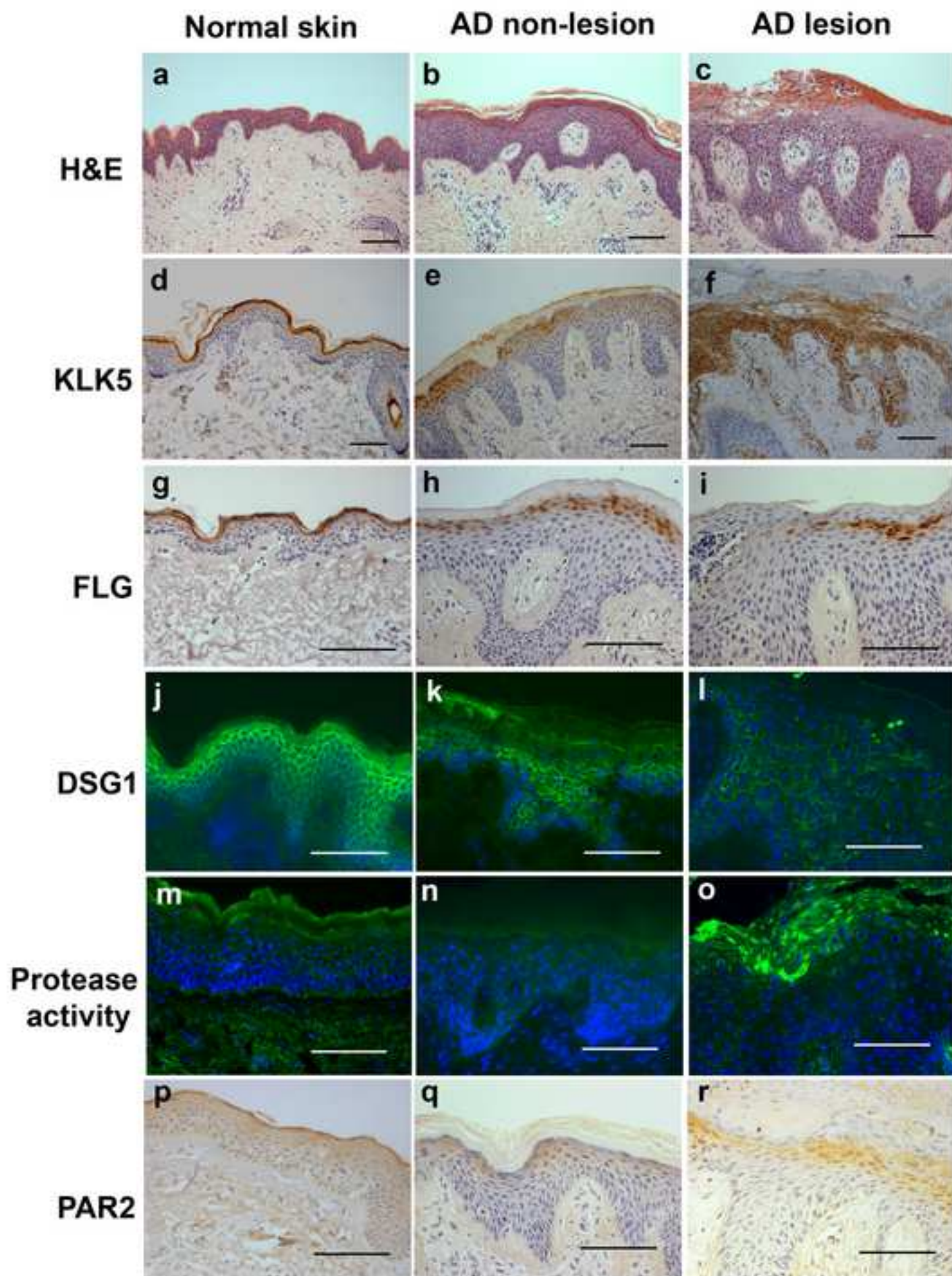


Figure 1B  
[Click here to download high resolution image](#)

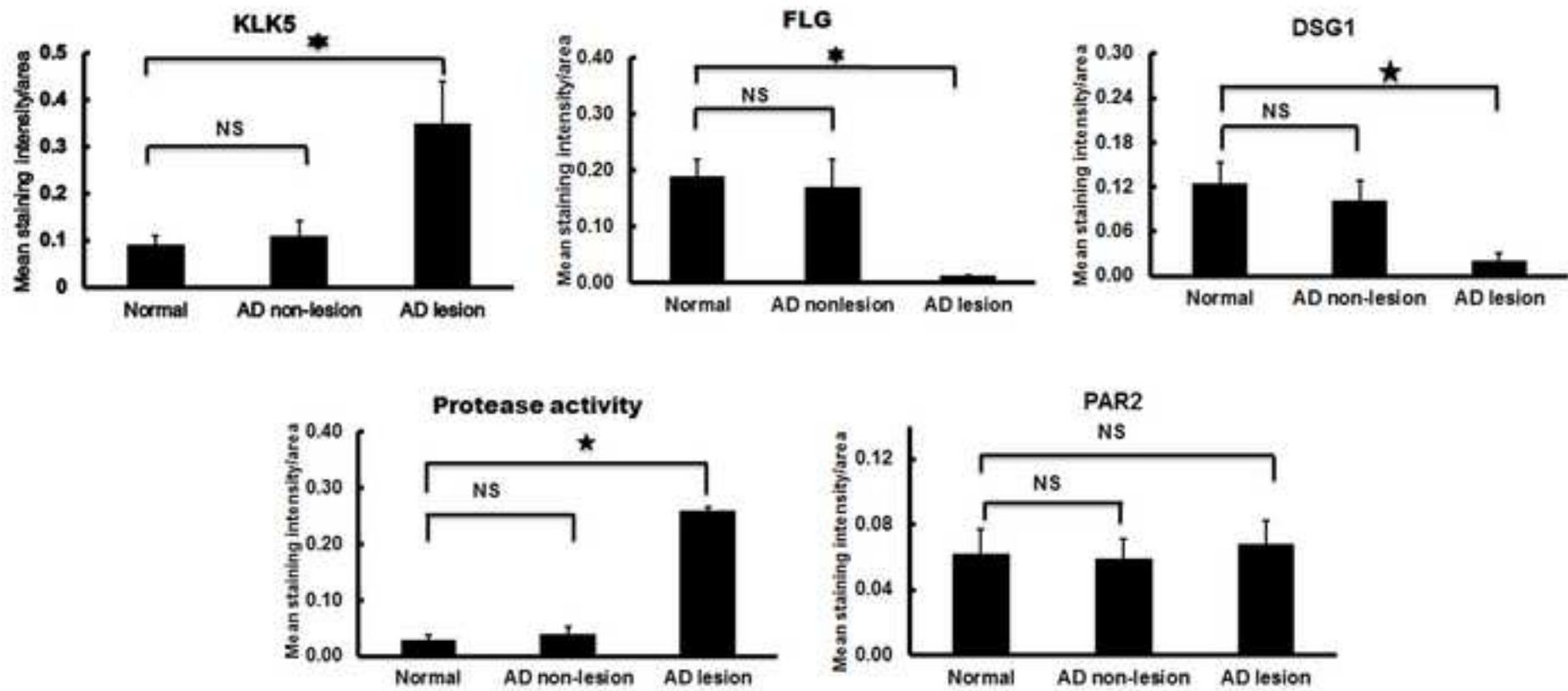




Figure 2

[Click here to download high resolution image](#)

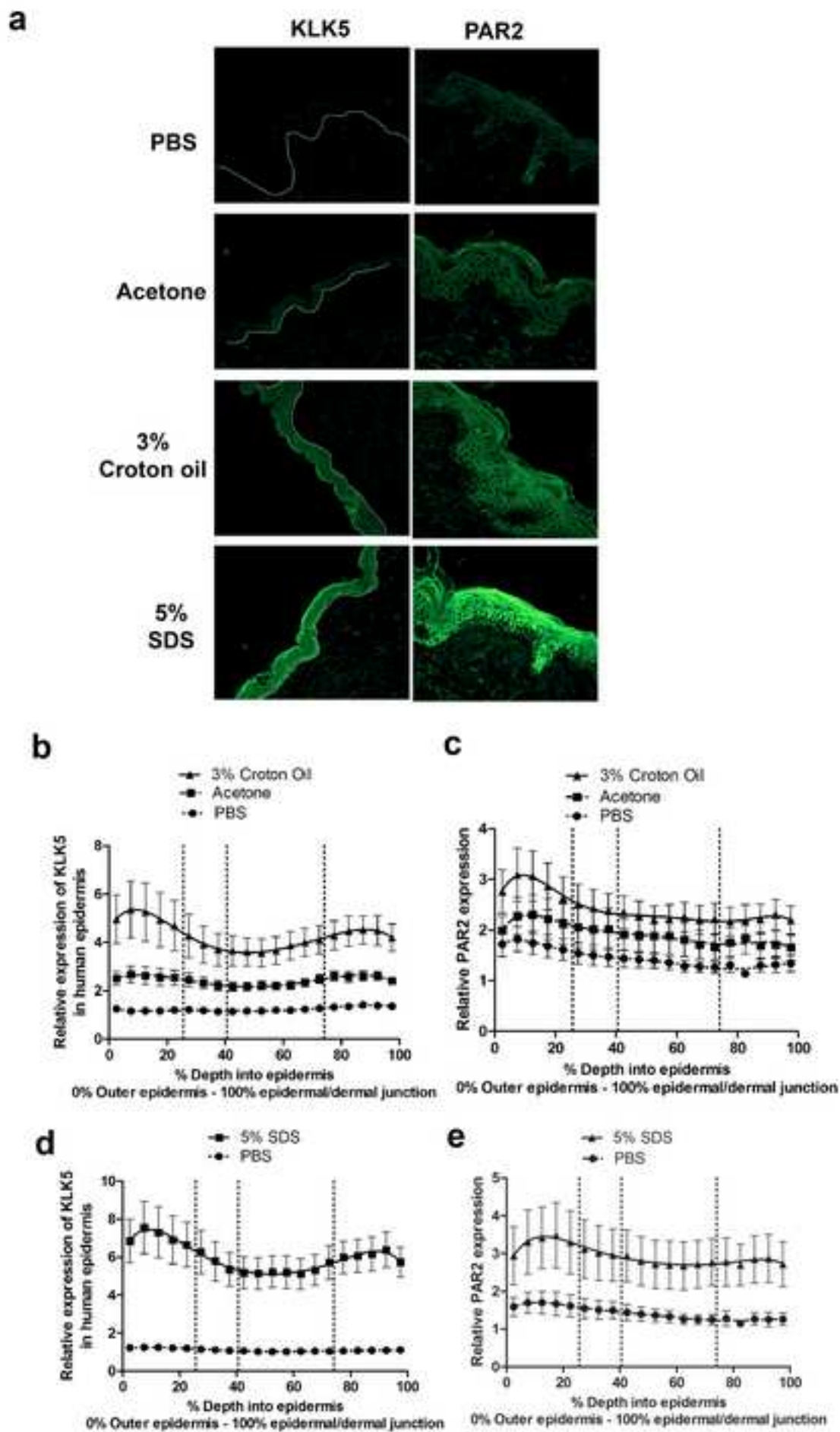


Figure 3

[Click here to download high resolution image](#)

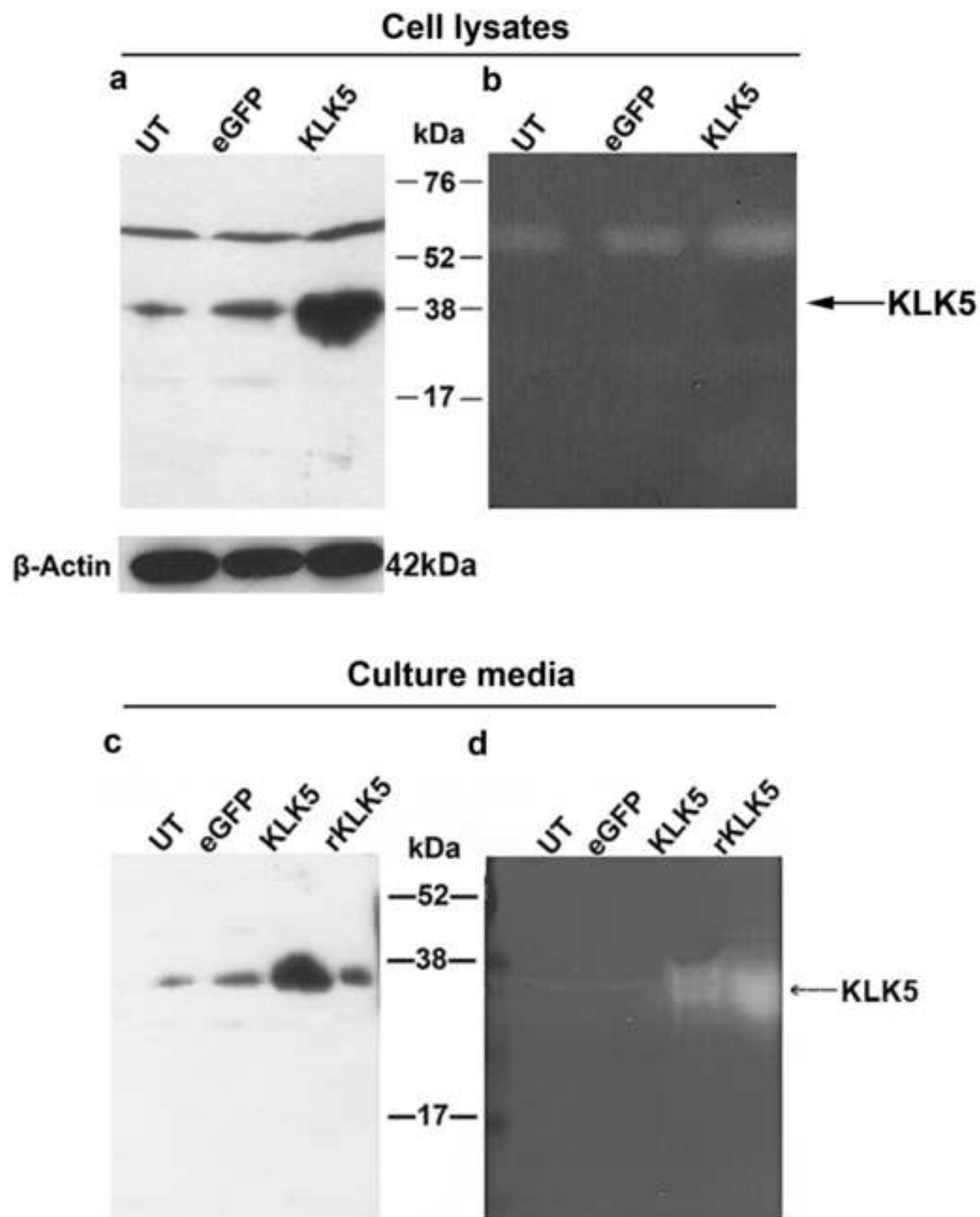
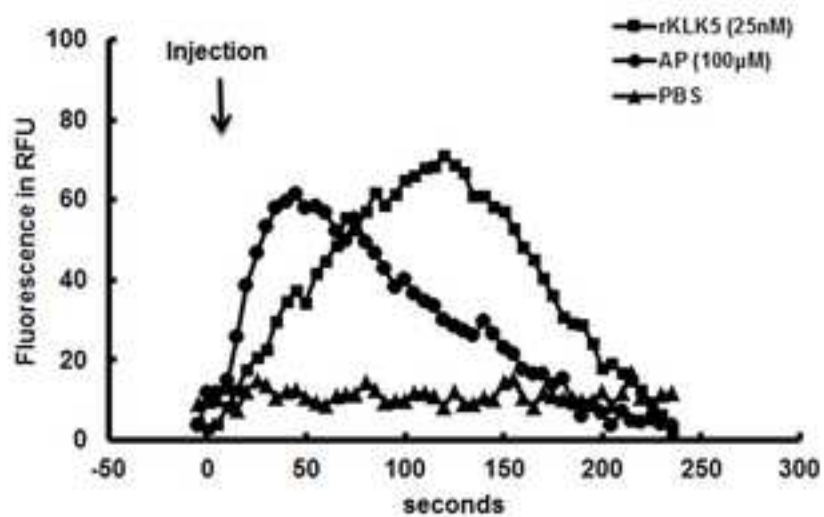


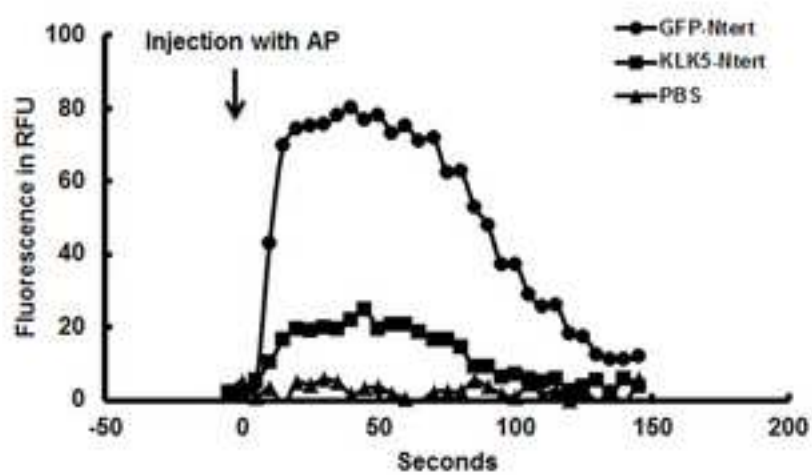
Figure 4

[Click here to download high resolution image](#)

**a**



**b**



**c**

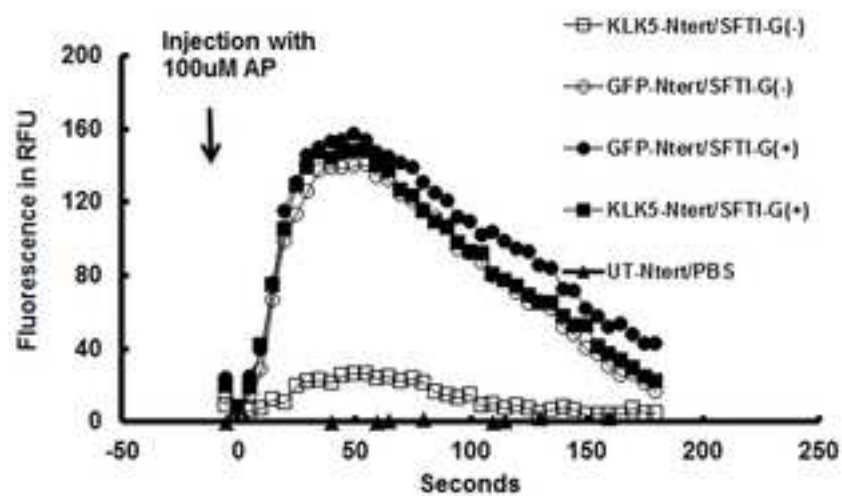
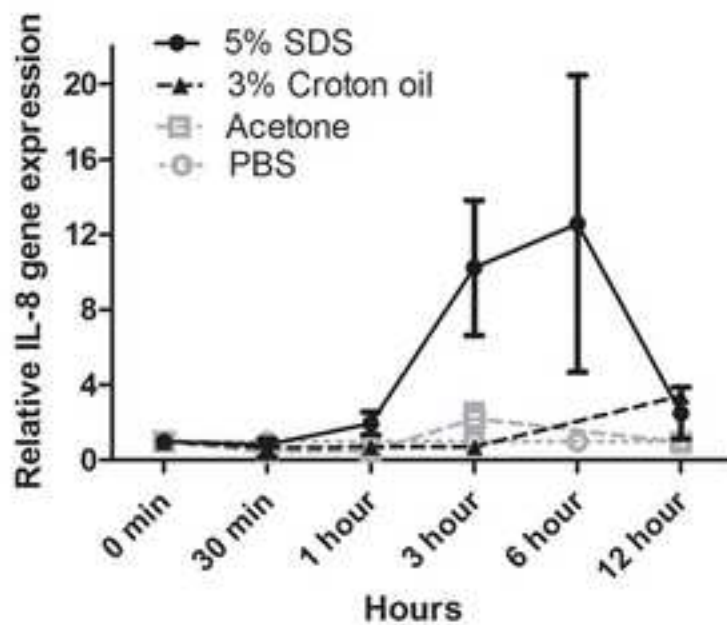
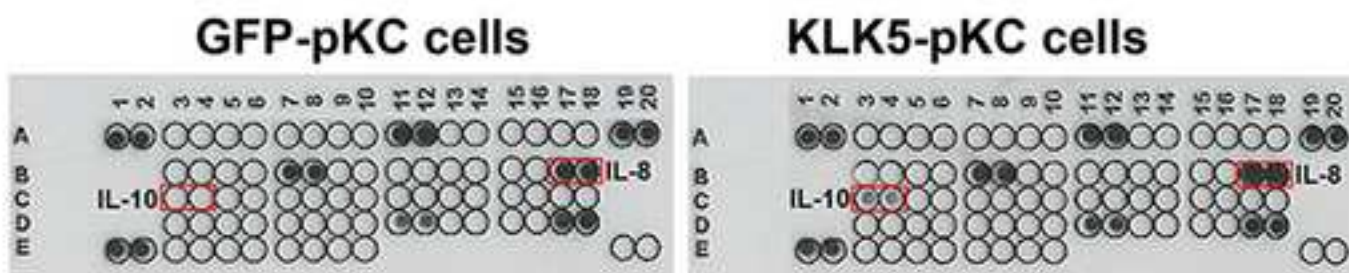


Figure 5  
[Click here to download high resolution image](#)

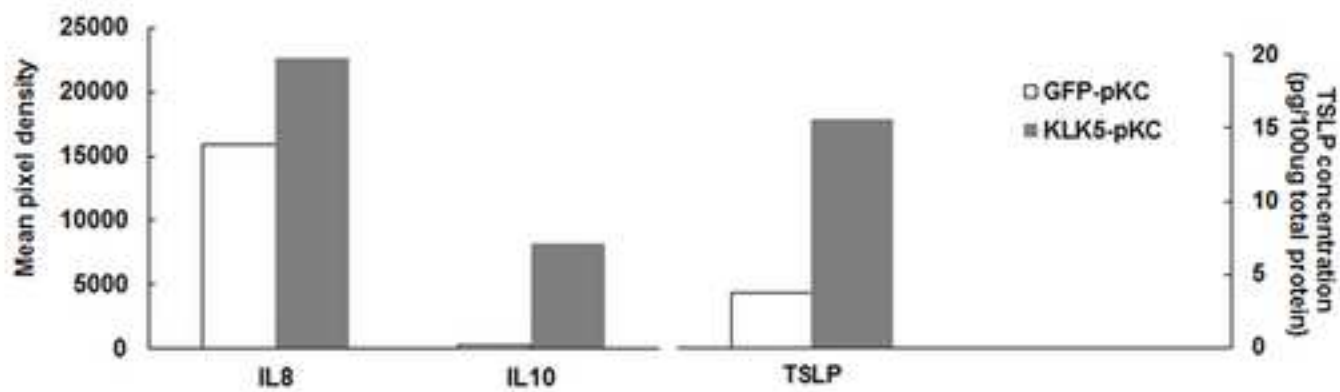
**a**



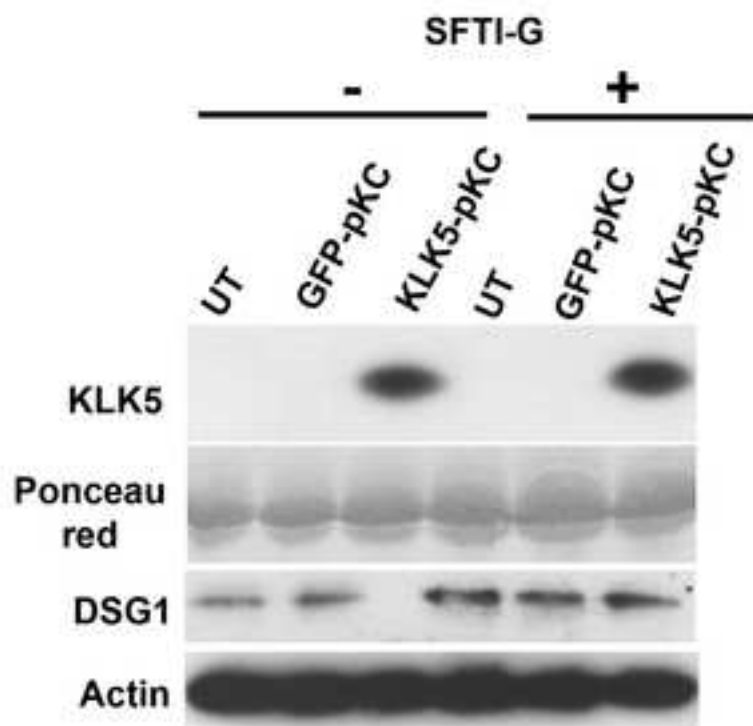
**b**



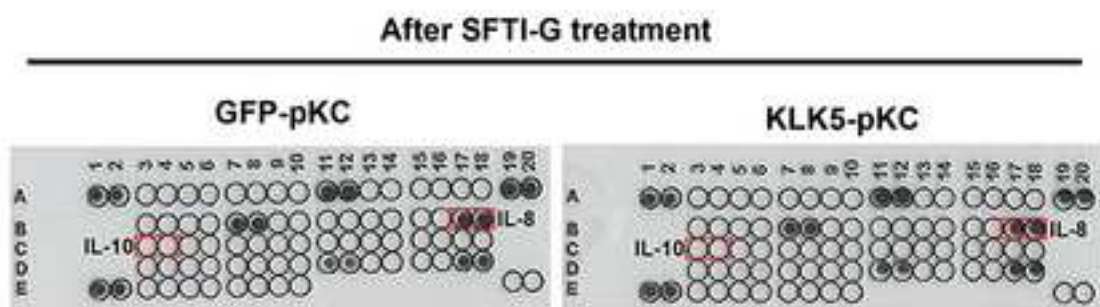
**c**



**a**



**b**



**c**

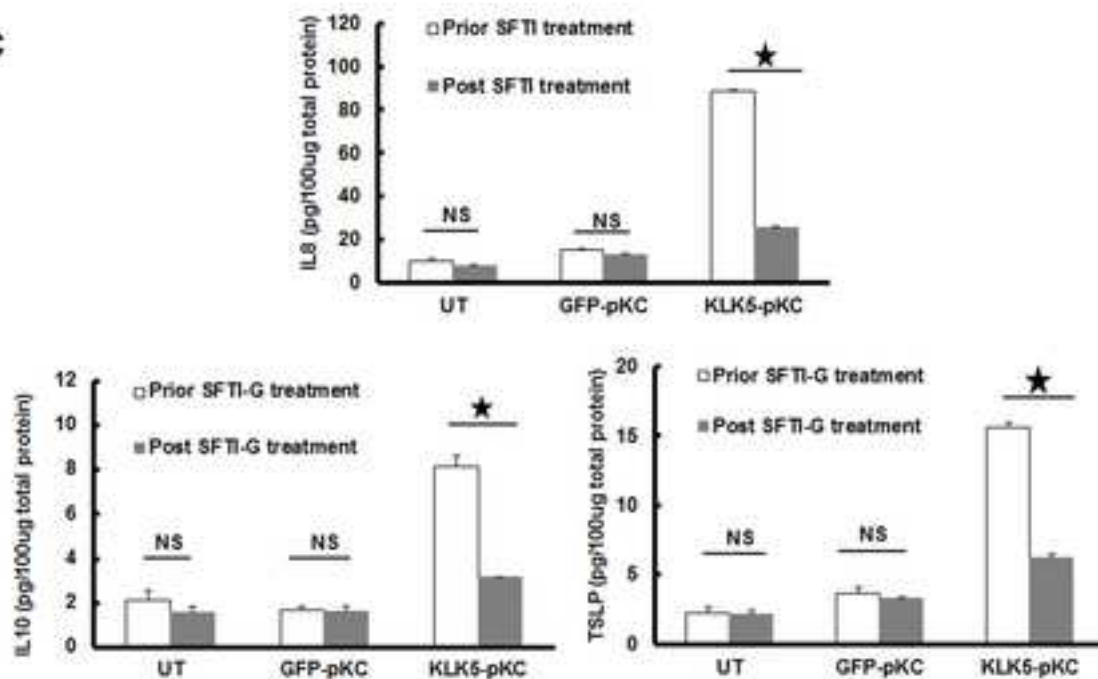


Figure 7  
[Click here to download high resolution image](#)

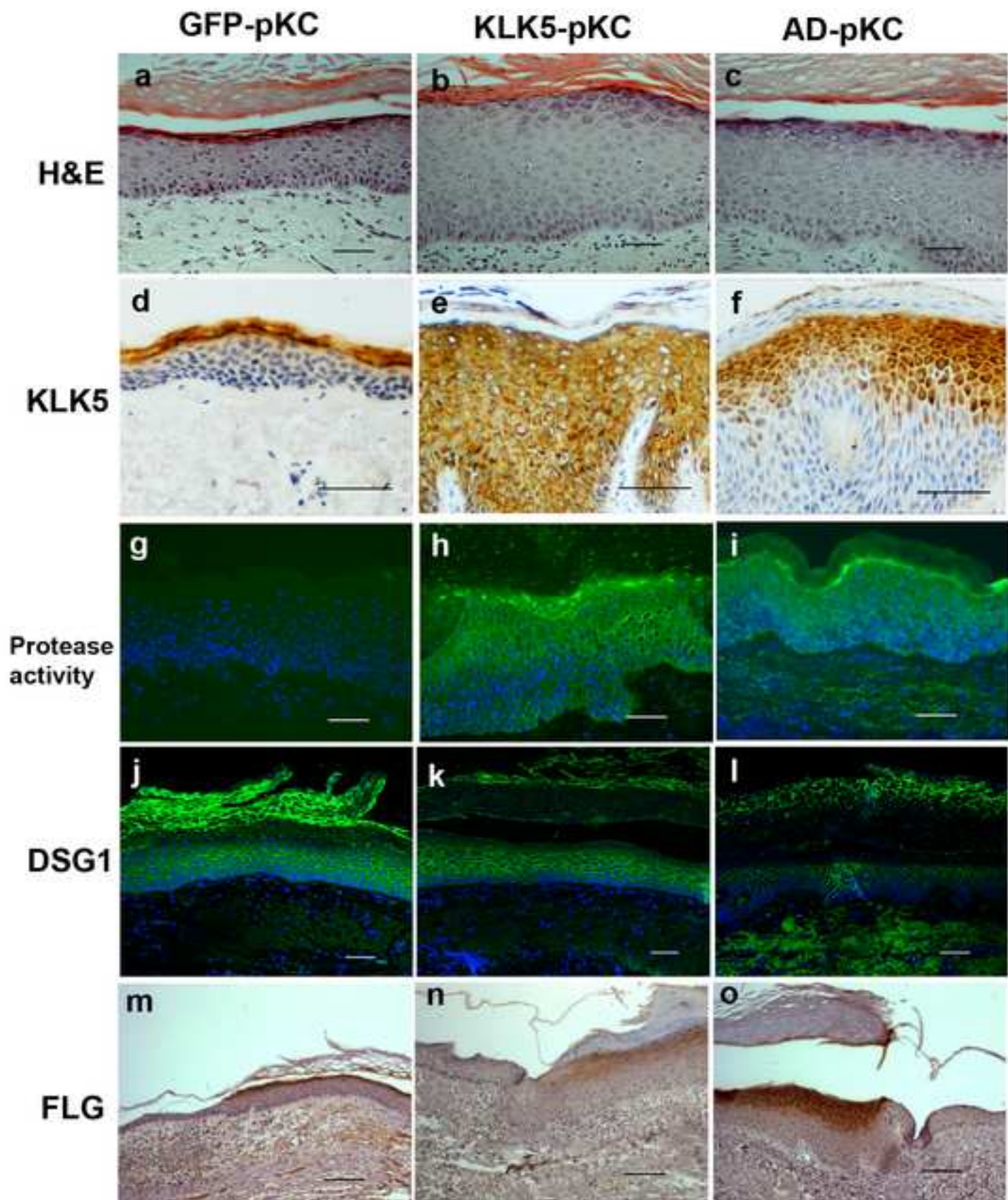


Figure S1

[Click here to download high resolution image](#)

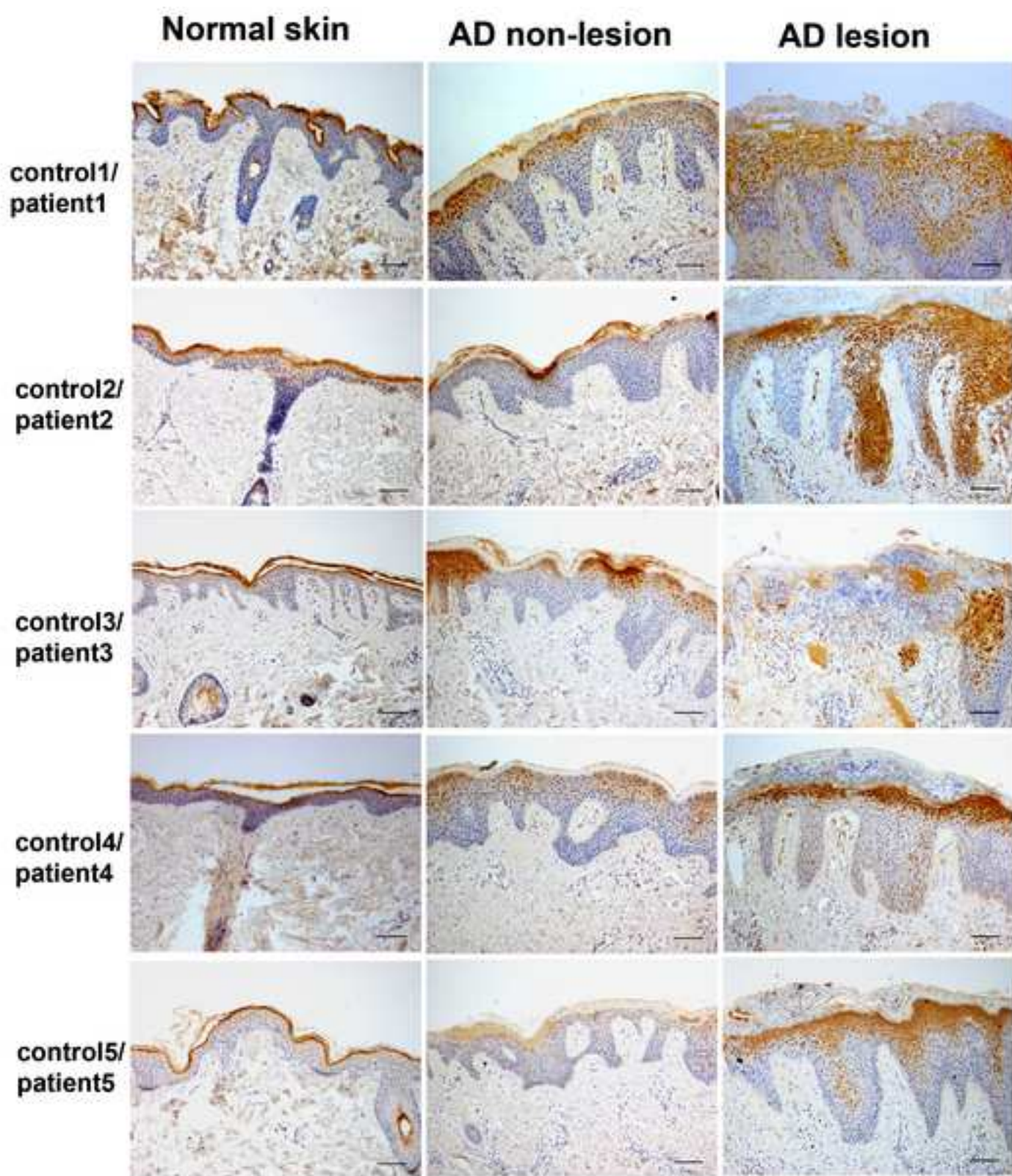


Figure S2

[Click here to download high resolution image](#)

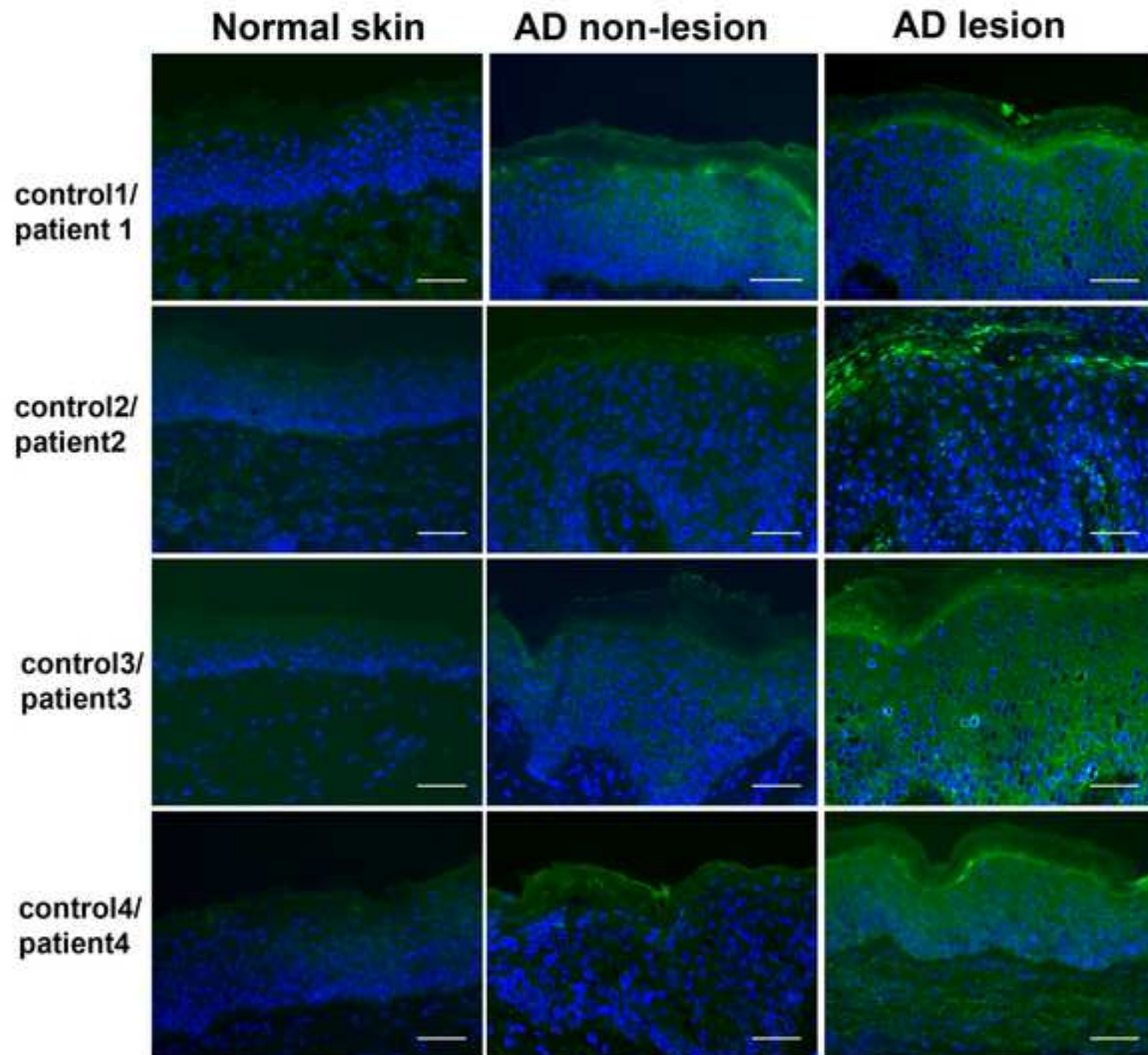




Figure S3  
[Click here to download high resolution image](#)

